16.8 An Integrated Magnetic Spectrometer for Multiplexed Biosensing

Constantine Sideris, Ali Hajimiri

California Institute of Technology, Pasadena, CA

There is high demand for at-home and point-of-care medical diagnostic tools as a step toward fast, low-cost, personal medicine. Integrated biosensors based on magnetic labeling schemes offer higher sensitivity and lower cost due to the elimination of the optics and have emerged as a viable alternative to assays that use fluorescence for biomolecular detection. For instance, the frequency-shift sensor of [1] demonstrates a high-sensitivity example of a cost-effective magnetic particle biosensor in CMOS with no need for external magnets. Despite their cost and sensitivity advantages, magnetic biosensors reported so far suffer from a lack of multi-probe diagnostics similar to fluorescent-based approaches that use multiple colors for simultaneous single-site multiple target differentiation. This is primarily because current approaches measure changes in the magnetic susceptibility, χ, either at low frequencies [2,3] or at a fixed RF frequency [1]. Consequently, these approaches do not provide a clear path for differentiating between a large number of small magnetic particles vs. a smaller number of larger size particles with similar magnetic content.

In the presence of an external alternating magnetic field, the rate at which magnetic domains can reorient to align with the external field is dependent on the domain size, with larger domains typically reorienting more slowly than smaller ones. This results in a frequency-dependent response in the magnetic susceptibility, χ [4]. As the frequency increases, the dipoles are limited by their finite reorientation speed, resulting in a decrease in χ due to a phase mismatch between the magnetic polarization vector, **M**(t) and the external magnetic field vector, **H**(t). In fact, there exists a resonance frequency, $f_{res,}$ at which the delay of the magnetic dipole is such that it completely cancels the field effect, resulting in χ=0. Interestingly, beyond $f_{res,}$, χ becomes negative and it eventually asymptotically approaches 0.

A crucial observation for our sensor is that f_{res} and the magnetic frequency spectrum ("signature") of the magnetic domains depend on the domain's size, and hence can be used as a spectroscopic means of differentiating between different kinds of beads that could be used for detecting different analytes. The typical shape of a magnetic susceptibility profile for paramagnetic nanoparticles is shown in Fig. 16.8.1 [4]. This phenomenon provides an effective means of single-site multiplexing in a CMOS magnetic sensor by using the spectroscopic data to discern between various beads similar to optical systems.

To enable multiple "multi-color" magnetic sensing schemes and take full advantage of the rich frequency-dependent information available, we design and demonstrate a CMOS magnetic spectrometer operating in a range of 1.1 to 3.3GHz (Fig. 16.8.2). Similarly to [1], the spectrometer requires no external biasing magnet or any exotic post-fabrication processing. Unlike prior results, the sensor operates at multiple frequencies over a diverse range and can be used without a reference sensor, effectively increasing its spatial multiplex density.
A frequency-shift sensing scheme is used to detect and measure magnetic materials. The sensor core is a stable free-running oscillator with on-chip LC resonators. The inductor of the LC tank is the magnetic-sensing cell, where its value changes due to the χ of the material. Thus, the full frequency-dependent information of χ is preserved by measuring the frequency shift due to magnetic materials on the sensor at frequencies of interest. The frequency tuning from 1.1 to 3.3GHz is achieved with a thermometer-coded switched-capacitor bank, allowing for 16 unique frequencies of operation within the range (Fig. 16.8.3). An NMOS-only differential cross-coupled topology is chosen and optimized for phase noise and power efficiency at 1.1GHz, since beads generally exhibit the largest response at this frequency [4]. Furthermore, the chip has two on-board 36b frequency counters and a digital divide-by-64 multiplexed output. As a demonstration of the ease of scalability of the system to a larger array, we implement a 4-sensor cell array (Fig. 16.8.3).

The oscillator achieves phase noise of -133.7dBc/Hz and -66.4dBc/Hz at 1MHz and 1kHz offsets respectively at 1.1GHz, and -124.8dBc/Hz and -43.2dBC/Hz at 1MHz and 1kHz offsets at 3.3GHz. The sensor core draws between 3 and 10mA depending on the adjustable current bias setting from a 0.6V supply and consumes as little as 1.8mW at the lowest current setting. The frequency signature of 1μm and 4.5μm Dynabeads beads from Invitrogen [6] and 1μm beads from Bangs Laboratories [7] are measured, as shown in Fig. 16.8.4. These beads are composed of magnetic nanoparticles within a polystyrene matrix and are coated with a biologically relevant functional group. To establish a concentration-independent standardized scale, the response at each frequency is normalized to that of the lowest frequency (1.1GHz). Figure 16.8.4 plots the mean of 3 measurements for each type of bead and demonstrates that there is greater variability in response at the higher frequencies mainly due to larger phase noise at higher frequency. Of note, the frequency response of each bead is dependent on the size and configuration of nanoparticles inside the polymer matrix, and not on the external size of the bead itself. Thus, it is not surprising the 1μm Bangs beads have a significantly different response from the 1μm Dynabeads. Since larger magnetic domains are expected to move slower and thus exhibit resonance at lower frequencies, this suggests that the Bangs beads have the largest nanoparticle size, while the 1μm Dynabeads have the smallest. This is consistent with the known nanoparticle sizes: Bangs estimate that their bead nanoparticle size is between 15 and 20nm (unpublished), which is larger than Dynabeads, which contain 5-to-8nm nanoparticles [5].

Multiplexed detection may be readily achieved by using beads with frequency signatures that are sufficiently orthogonal. An evaluation of the sensor's multiplexing capability is performed by measuring the frequency responses of a series of density-constant (10mg/ml) colloids containing differing ratios of 1μm DynaBeads to 1μm Bangs beads. Seven mixtures of Dynal and Bangs beads are evaluated at proportions: [D% : B%]: 100:0, 87.5:12.5, 75:25, 50:50, 25:75, 12.5:87.5, 0:100. Three measurements were taken of each sample and averaged to reduce the effects of variability in spotting of beads on the sensor cells. Measurements were taken after the bead solutions had dried on the sensor surface. Each measurement was taken over a 2-minute period to allow stabilization of the frequency after bead placement. Figure 16.8.5 shows the averaged frequency signatures of all the mixtures. Using the data from Fig. 16.8.4 as basis vectors and taking the different standard deviations at each frequency into account, we perform a σ-weighted GLS analysis to predict the proportions of each bead present in each sample and plot the results against the known exact proportions in Fig. 16.8.6. The results clearly demonstrate the magnetic multiplexing of different beads indicating the viability of the sensor for complicated bioassays requiring multiple marker types.

The biosensor is implemented in a 65nm CMOS process. Each sensing site is 260×260μm, a surface area sufficient for protein or DNA detection experiments with detectable bead binding capacity. The full size of the four-sensor chip is 1.2×1.2mm.

Acknowledgements:
The authors thank the members of Caltech CHIC and MICS group for technical discussions, Yun E. Wang for assistance in sample preparation, and ST Microelectronics for chip fabrication. This material is based upon work supported by the National Science Foundation Graduate Research Fellowship under Grant No. DGE-1144469.

References:
[1] H. Wang, *et al.*, "A Frequency-Shift CMOS Magnetic Biosensor Array with Single-Bead Sensitivity and No External Magnets," *ISSCC Dig. Tech. Papers*, Feb. 2009.
[2] S. Han, *et al.*, "A High-Density Magnetoresistive Biosensor Array with Drift-Compensation Mechanism," *ISSCC Dig. Tech. Papers*, Feb. 2007.
[3] P. Besse, *et al.*, "Detection of A Single Magnetic Microbead Using a Miniaturized Silicon Hall Sensor," *Appl. Phys. Letters*, vol. 80, no. 22, pp. 4199-4201, June 2002.
[4] PC Fannin, *et al.* "Investigation of the Complex Susceptibility of Magnetic Beads Containing Maghemite Nanoparticles," *J. Mag. and Mag. Mat.* vol. 303, pp. 147-152, Dec. 2005.
[5] Geir Fonnum, *et al.*, "Characterisation of Dynabeads by Magnetization Measurements and Mossbauer Spectroscopy," *J. Mag. and Mag. Mat.*, vol. 293, pp. 41-47, Mar. 2005.
[6] http://www.invitrogen.com, [online] accessed Nov. 17, 2012.
[7] http://www.bangslabs.com, [online] accessed Nov. 17, 2012.

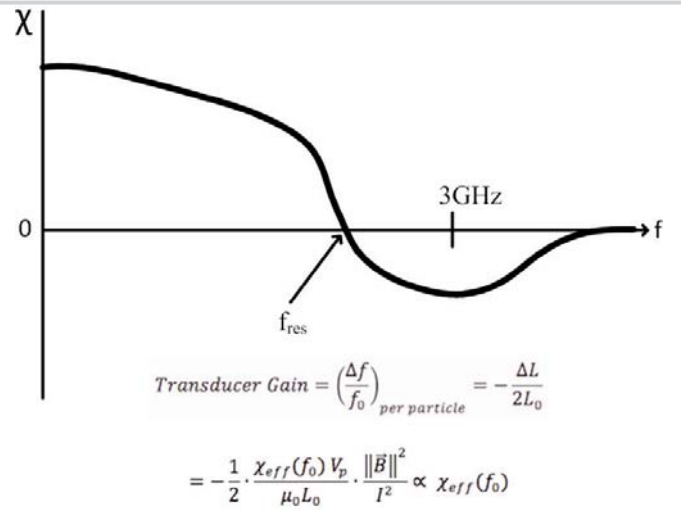

Figure 16.8.1: Typical frequency dependence curve of χ for magnetic nanoparticles. Sensor response at each frequency is proportional to χ at that frequency.

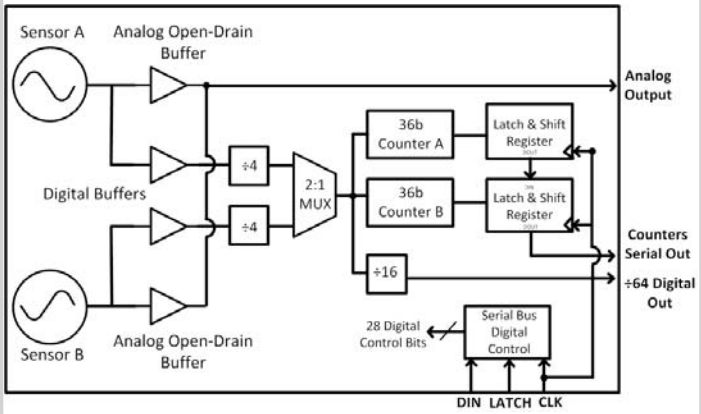

Figure 16.8.2: System block diagram: a 2-sensor unit block is shown, whereas the full implementation has 4 cells.

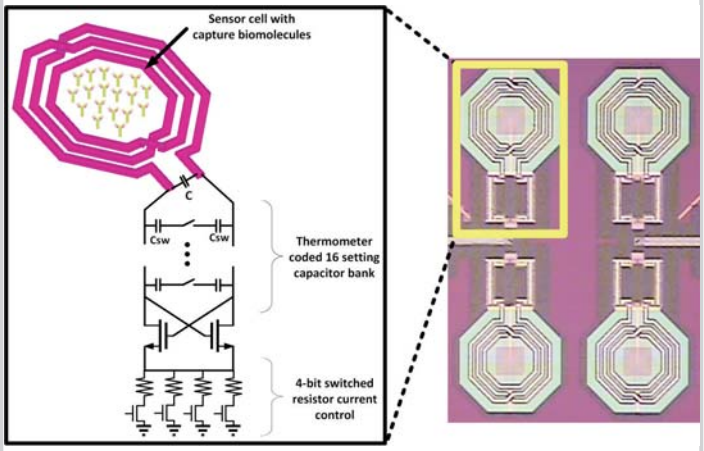

Figure 16.8.3: Sensor cell schematic and die photo.

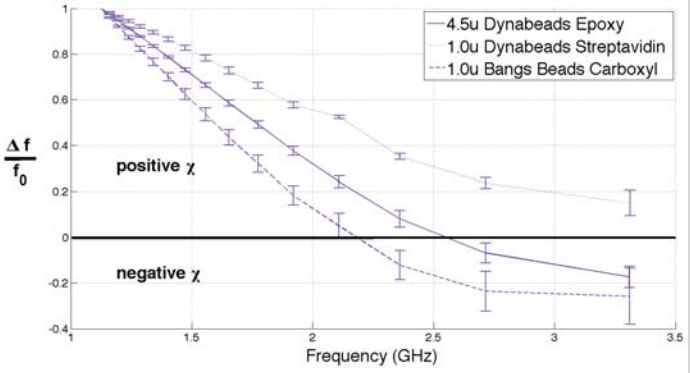

Figure 16.8.4: Frequency response measurement of three different kinds of beads. Error bars represent one standard deviation around the mean across 3 measurements for each bead type.

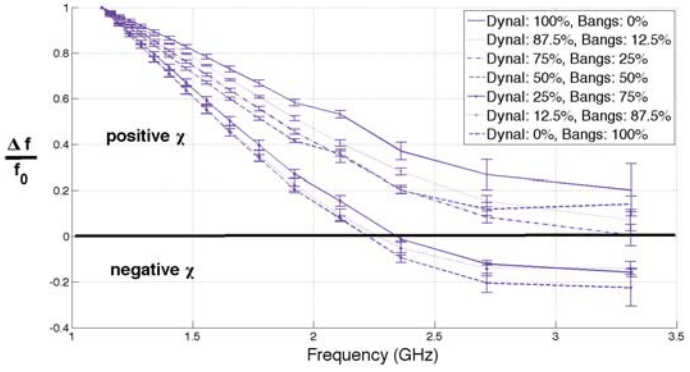

Figure 16.8.5: Spectroscopic measurements of mixtures of various proportions of Dynal and Bangs 1μm beads.

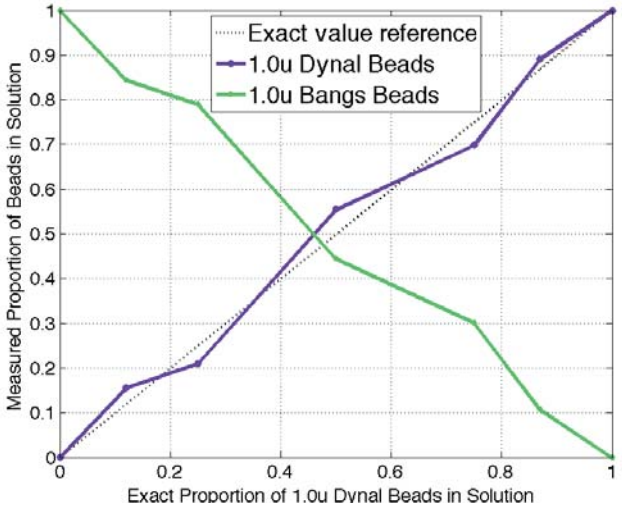

Figure 16.8.6: Measured proportion of beads from data of Fig. 16.8.5 for different rations: [D%, B%]: 100:0, 87.5:12.5, 75:25, 50:50, 25:75, 12.5:87.5, 0:100.

16

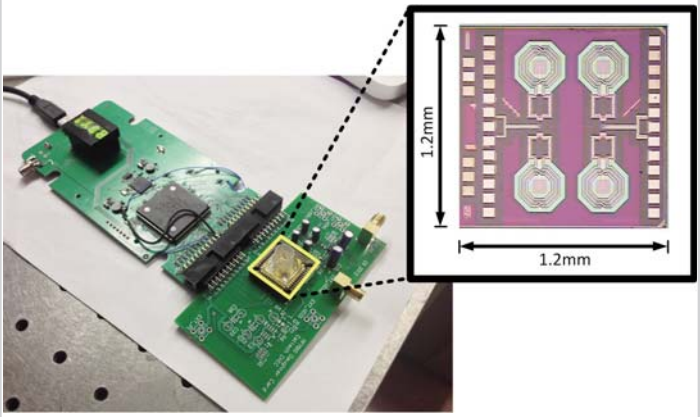

Figure 16.8.7: Handheld USB powered measurement setup with die photo of 2x2 sensor array.

978-1-4673-4516-3/13/$31.00